

Calculation of rates of exciton dissociation into hot charge-transfer states in model organic photovoltaic interfaces

Héctor Vázquez* and Alessandro Troisi†

Department of Chemistry and Centre of Scientific Computing, University of Warwick, Coventry CV4 7AL, UK

(Received 1 July 2013; published 12 November 2013)

We investigate the process of exciton dissociation in ordered and disordered model donor/acceptor systems and describe a method to calculate exciton dissociation rates. We consider a one-dimensional system with Frenkel states in the donor material and states where charge transfer has taken place between donor and acceptor. We introduce a Green's function approach to calculate the generation rates of charge-transfer states. For disorder in the Frenkel states we find a clear exponential dependence of charge dissociation rates with exciton-interface distance, with a distance decay constant β that increases linearly with the amount of disorder. Disorder in the parameters that describe (final) charge-transfer states has little effect on the rates. Exciton dissociation invariably leads to partially separated charges. In all cases final states are “hot” charge-transfer states, with electron and hole located far from the interface.

DOI: [10.1103/PhysRevB.88.205304](https://doi.org/10.1103/PhysRevB.88.205304)

PACS number(s): 71.35.-y, 72.80.Lc, 73.50.Pz, 88.40.jr

I. INTRODUCTION

In organic photovoltaic cells incident light creates bound electron-hole (e-h) pairs. The generation of free holes and electrons takes place between an electron-donor material (often the light absorber) and an electron-acceptor material. The process of generating free holes and electrons in donor and acceptor materials from an exciton localized in one of them is one of the most crucial phenomena in organic solar cells yet possibly one of the least understood. A common explanation is that the bound exciton in the donor dissociates into a strongly bound e-h pair localized at the interface between donor and acceptor.¹ However, it is not easy to explain how free charges can be formed from such a stable pair in the subpicosecond time scales observed experimentally^{2,3} in such a low dielectric constant medium.⁴⁻⁶ Several mechanisms have been proposed to explain the separation of the bound e-h pair into free charges, such as the excess energy generated in the formation of the bound e-h pair,⁶ the effect of intrinsic dipoles at the donor/acceptor interface,^{7,8} or the delocalization of charge carriers along the polymer chains.⁹ However, no clear consensus exists today.^{6,10-13} At the same time, a growing number of recent publications have highlighted the important role of higher-energy excitonic charge-transfer states. “Hot” excitons having excess energy with respect to the bound e-h pair have been shown to dissociate with high efficiency.¹³⁻¹⁷ The reason is that these “hot” charge-transfer (CT) states have e-h separations that are significantly larger than those of the interface bound e-h pair.

In this paper we describe exciton dissociation as a purely electronic resonant process and do not include polaronic effects, an assumption further discussed below. We consider a widely applicable model Hamiltonian of donor/acceptor interfaces and calculate the generation rate of CT states from initial Frenkel states in the donor material. We focus on the delocalization of the initial excitonic states and analyze in a controlled way the influence of static disorder in the initial or final states on the generation rate of CT states.

II. THEORETICAL MODEL

We describe the donor/acceptor interface as a one-dimensional system [Fig. 1(a)] of N donor and N acceptor

sites. In our model there are two possible sets of states, which describe the initial and final states of the exciton dissociation process. Initial states are Frenkel excitons, whereas final states are CT states, with the hole located on the donor sites and the electron on the acceptor. Frenkel states are localized excitations where electron and hole reside in the same donor site. We describe Frenkel states in the donor chain by a linear combination of localized excitations.¹⁸ We adopt the notation of labeling donor sites i and acceptor sites j [Fig. 1(a)], with i and j equal to 1 at the interface.

The Hamiltonian for Frenkel states, which reside in the donor material, is

$$\hat{H}_F = \sum_i E_{\text{ex}}^i |i\rangle \langle i| + \sum_i J^i |i\rangle \langle i+1| + \text{H.c.}, \quad (1)$$

where E_{ex}^i and J^i are the on-site energy and the nearest-neighbor coupling for the exciton. For perfectly ordered systems (one of the limits considered) all exciton site energies and couplings are the same $E_{\text{ex}}^i = E_{\text{ex}}$, $J^i = J$. In CT states $|i, j\rangle$, positive and negative charges reside in the donor i and acceptor j sites, respectively. The Hamiltonian for the CT states is

$$\begin{aligned} \hat{H}_{\text{CT}} = & \sum_{i,j} -\frac{C}{n_{ij}} |i, j\rangle \langle i, j| + \sum_{ij} V_A^j |i, j\rangle \langle i, j+1| \\ & - \sum_{ij} V_D^i |i, j\rangle \langle i+1, j| + \text{H.c.}, \end{aligned} \quad (2)$$

where $C = \frac{e^2}{4\pi\epsilon R_0}$ is the Coulomb energy of an electron and hole at neighboring sites, and V_D^i and V_A^j are the hole and electron hopping terms at donor site i and acceptor site j , respectively.¹³ $\frac{C}{n_{ij}}$ is the Coulomb energy of a hole at donor site i and an electron at acceptor site j , separated by n_{ij} sites.

Electronic coupling between Frenkel and CT states takes place at the interface between donor and acceptor. From configuration interaction theory this coupling can be approximated¹³ by the nearest-neighbor Fock matrix element V_{DA} between the LUMOs of the donor and acceptor at the interface sites. We therefore model this coupling as a nearest-neighbor term V_{DA}

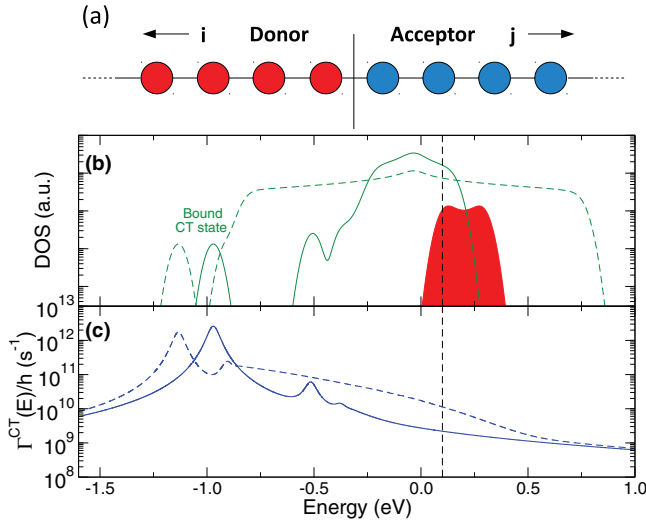


FIG. 1. (Color online) (a) One-dimensional donor/acceptor model used in this paper. The donor site index i runs to the left of the figure, away from the acceptor. (b) Density of states of Frenkel states (red) and CT states (green) neglecting the interaction between them for two different parameters $V_A = V_D = 0.05$ eV (solid line) and $V_A = V_D = 0.2$ eV (dashed line). (c) $\Gamma_{nn}^{\text{CT}}(E)/h$ for the lowest Frenkel state $n = 1$ as a function of energy, for the same parameters as (b). Peaks in the $\Gamma^{\text{CT}}(E)$ curve correspond to features in the isolated CT DOS. The vertical dashed line shows the energy of the lowest Frenkel state.

between states $|i = 1\rangle$ (Frenkel) and $|i = 1, j = 1\rangle$ (CT); i.e.,

$$\hat{H}_V = V_{DA} |i = 1\rangle \langle i = 1, j = 1| + \text{H.c.} \quad (3)$$

The total Hamiltonian is then the sum of the isolated Frenkel and CT Hamiltonians and the coupling term:

$$\hat{H} = \hat{H}_F + \hat{H}_{\text{CT}} + \hat{H}_V. \quad (4)$$

We use Green's function methods to calculate exciton dissociation rates. The large number of closely spaced CT states approaches a continuum. In similarity with molecular transport methods, we project the CT states onto the Frenkel Hamiltonian by means of a self-energy operator.^{19,20} This implies describing the interaction of the CT states through an effective non-Hermitian, energy-dependent (self-energy) potential acting on the Frenkel states. We work with an effective Hamiltonian

$$\hat{H} = \hat{H}_F + \hat{H}_{\text{CT}} + \hat{H}_V \rightarrow \hat{H}_{\text{eff}} = \hat{H}_F + \Sigma^{\text{CT}}(E), \quad (5)$$

where $\Sigma^{\text{CT}}(E)$ is the CT self-energy. This not only avoids the manipulation of the CT Hamiltonian H_{CT} (of size N^2 , consistent with CT states requiring two indices) but also allows us to easily extract the generation rate of CT states. If we label n (m) the eigenstates of the Frenkel (CT) Hamiltonians, we calculate this self-energy operator from the Green's function of the isolated CT states $g^{\text{CT}}(E) = \sum_m (E - \epsilon_m + i\eta)^{-1}$ with $\eta \rightarrow 0^+$ and from the coupling between Frenkel and CT states V_{nm} as

$$\Sigma_{nn'}^{\text{CT}}(E) = \sum_m V_{nm} g_{mm'}^{\text{CT}}(E) V_{mn'}^\dagger. \quad (6)$$

We expand the Frenkel and CT states on the site basis as $|\Psi_n^F\rangle = \sum_i d_i^n |i\rangle$, $|\Psi_m^{\text{CT}}\rangle = \sum_{i,j} c_{ij}^m |i,j\rangle$. Then

$$\Sigma_{nn'}^{\text{CT}}(E) = \sum_m |V_{DA}|^2 d_1^n d_1^{n'} |c_{11}^m|^2 g_{mm}^{\text{CT}}(E). \quad (7)$$

The self-energy is proportional to the square of the coupling V_{DA}^2 , as expected.^{19,20} There is an explicit energy dependence through the isolated CT Green's function $g^{\text{CT}}(E)$. Finally, since the coupling between Frenkel and CT states takes place at the interface ($i = 1, j = 1$), the self-energy is modulated by the coefficients of these states at the interface.

The real and imaginary parts of the self-energy are related to the shift in on-site energy and lifetime, respectively, of Frenkel states^{19,20} due to their interaction with the CT manifold. In particular, for a Frenkel state n the quantity $\Gamma_{nn}^{\text{CT}}(E)$ is inversely proportional to its lifetime τ_n and is given by

$$\Gamma_{nn}^{\text{CT}}(E) = \frac{\hbar}{\tau_n} = i [\Sigma_{nn}^{\text{CT}}(E) - \Sigma_{nn}^{\text{CT}\dagger}(E)]. \quad (8)$$

The energy-dependent term $\Gamma_{nn}^{\text{CT}}(E)$ reflects the fact that the spectral features of Frenkel states n are broadened due to their coupling with CT states.

This expression for the dissociation rate is consistent with the Marcus equation²¹ generally used to describe nonadiabatic electron transfer processes. In the limit of ultrafast processes or large clusters, where dissociation can be treated as a resonant electronic process and polaronic effects can be neglected, the Marcus rate reduces to Eq. (8).

III. ORDERED DONOR/ACCEPTOR INTERFACES

We first consider the situation of perfectly ordered donors and acceptors. Figure 1(b) shows the density of states (DOS) of the Frenkel and CT systems neglecting the interaction between them for a system of $N = 30$ donors and 30 acceptors, with the following parameters: $E_{\text{ex}} = 0.2$ eV, $J = 0.05$ eV, $V_A = V_D = 0.05$ eV (solid line), $V_A = V_D = 0.2$ eV (dashed line), $V_{DA} = 0.5$ eV, $C = 0.96$ eV.³⁵ In our model zero energy corresponds to the dissociated charges separated at infinite distance. The Frenkel parameters have been chosen so that the lowest Frenkel state (at $E_{\text{ex}} - 2J$) lies slightly above zero in order for charge separation to be thermodynamically favored. The dashed vertical line in Figs. 1(b) and 1(c) marks the energy of the lowest Frenkel state. The Frenkel and CT DOS curves have been obtained with a 30 meV Gaussian broadening.

The CT DOS is dominated by a broad band peaked at $E \simeq 0$, whose width is determined by V_A and V_D . Well separated from this band at $E \sim -1.0$ eV is the CT bound state. This is the well-documented bound CT state¹⁰ corresponding to the electron and hole being strongly localized at the interface by Coulomb attraction and having a small electron-hole (e-h) separation (~ 1 site). Other bound, less localized states having larger e-h separations ($\lesssim 10$ sites) can lie at higher energies,²² while the states at the center of the CT band are fully delocalized. These are the states degenerate with the initial Frenkel states, which cause their broadening and are the CT states the Frenkel states dissociate into.

The degeneracy between the initial electronic state and the manifold of continuum CT states makes dissociation very fast, suggesting it is an essentially (resonant) electronic process,

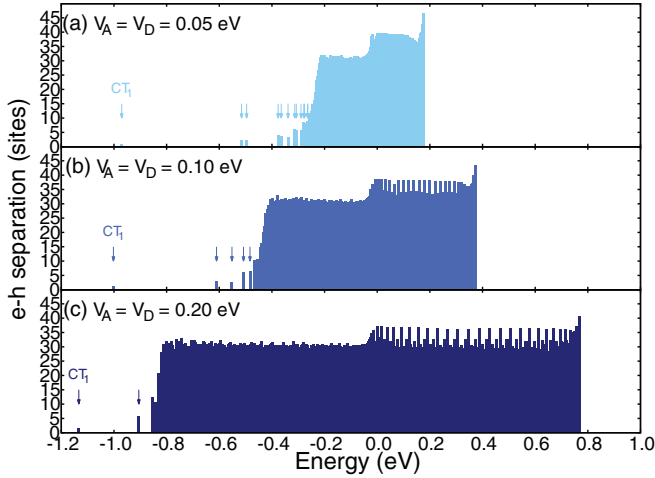


FIG. 2. (Color online) Electron-hole (e-h) separation of CT states as a function of energy in a system of 30 donor and 30 acceptors for the different values of the CT band parameters indicated. The arrows show CT states below the band which have an e-h separation of less than 10 sites. The bound geminate CT_1 state localized at the interface is at $E \sim -1$ eV.

where nuclear degrees of freedom do not play a major role. The coupling with the nuclear degrees of freedom becomes important for regimes where a small polaron can be formed, a situation uncommon for high-performance polymeric²³ or molecular²⁴ semiconductors. An illustration of how the inclusion of polaronic effects does not alter the nature of the initial and final states is given for example in Ref. 13.

We consider for example the lowest Frenkel state ($n = 1$) and study exciton dissociation rate at the bottom of the Frenkel band at an energy of ~ 0.1 eV [shown in Figs. 1(b) and 1(c) by a vertical dashed line]. Figure 1(c) shows the broadening $\Gamma_{n=1, n=1}^{CT}(E)/h$ of the lowest Frenkel state as a function of energy. The features in these curves follow closely the shape of the CT DOS. Larger values of V_A and V_D increase the CT bandwidth and result in slightly higher values near $E = 0$. On the other hand, the coupling between Frenkel and CT excitons V_{DA} does not affect the shape of the dissociation curve but instead scales the rates through $|V_{DA}|^2$, as seen in Eqs. (7) and (8).

In ordered donor/acceptor systems, where Frenkel states are delocalized across the donor chain, dissociation rates can be high. In particular, for a certain range of values of the parameters, especially N and V_{DA} , exciton dissociation rates are of the order of $\sim 10^{10}$ s⁻¹. Since dissociation, in this electronic resonant process, takes place at energies within the CT band, we find that final (CT) states are partially separated e-h states.

Figure 2 shows the e-h separation of CT states (eigenstates of H_{CT}) as a function of energy for three different values of the CT parameters V_A, V_D , for a system of $N = 30$ donor and $N = 30$ acceptor sites. Larger values of V_A and V_D result in a wider CT band. The e-h separation was calculated by weighing over the charge density on the donor and acceptor sites. For a CT state $|\Psi_m^{CT}\rangle = \sum_{i,j} c_{ij}^m |i,j\rangle$, its e-h separation is

$$d_{e-h}^m = \sum_{i,j} (i+j-1) |c_{ij}^m|^2, \quad (9)$$

where, since both donor and acceptor indices start at 1 ($i, j = 1, 2, \dots, N$), the distance between sites i and j is defined as $n_{ij} = i + j - 1$, so that it is equal to 1 for interface donor/acceptor sites ($i = j = 1$). Notice that the e-h separation within the CT band is of the order of the donor or acceptor chain length. Knowledge of the states generated by ultrafast exciton dissociation can be also used as a first step for the calculation of the subsequent thermalization of the carrier that may lead either to free charges (possible only in a semi-infinite) or bound e-h pairs. This aspect is not considered by the present paper.

Expectedly, the results presented so far for the perfectly ordered system are affected by the size of the model. For larger model systems the Frenkel exciton becomes more diluted and less coupled to the CT manifold. The changes are not very large. Compared to $N = 30$, reducing (increasing) the size of the donor and acceptor chains by 10 increases (reduces) the dissociation rates by a factor ~ 3 .

IV. DISORDERED DONOR/ACCEPTOR INTERFACES

Static disorder in organic materials can have multiple origins (e.g., electrostatic disorder in small molecules²⁵ or conformational disorder in polymers²⁶) and invariably causes localization of excitonic and charged states. It has been proposed that the different degrees of disorder at the interface may change the efficiency of exciton dissociation.^{27–29} We introduce disorder in our model by generating a Hamiltonian where its parameters (e.g., E_{ex}^i) are drawn (uncorrelated) from a Gaussian distribution centered at their reference values (i.e., without disorder, E_{ex}) and whose standard deviation σ is changed. The amount of disorder in a parameter X is quantified through the value of the standard deviation relative to the ideal value σ_X/X . By introducing disorder in each parameter (e.g., $X = E_{ex}$) independently of the others (J, V_A, V_D) we evaluate the effect of disorder in a controlled way. We generate many disordered donor/acceptor “samples” in this manner.

We start by considering the effect of disorder in parameter E_{ex}^i , focusing on the dissociation rate of the lowest Frenkel state $|\Psi_{n=1}^F\rangle = \sum_i d_i^{n=1} |i\rangle$. The average position of such exciton is given by $i^{av} = \sum_i i |d_i^{n=1}|^2$ and the degree of localization is measured by the participation ratio $PR_F = 1/\sum_i |d_i^{n=1}|^4$ (a measure of how many donor sites the Frenkel state is delocalized over).

In the absence of disorder, the lowest Frenkel state is given by the analytical solution to the Frenkel Hamiltonian [Eq. (1)] and is simply the sine wave $|\Psi_{n=1}^F\rangle = \sqrt{2/(N+1)} \sum_i \sin(k_1 i) |i\rangle$ with $k_1 = \pi/(N+1)$, where i labels the donor sites and N is the number of sites in the donor chain ($N = 30$ in this paper). The participation ratio can be obtained analytically and is found to be $\frac{2}{3}(N+1)$, comparable to the length of the donor and acceptor chains.

For ideal donor materials, with no disorder, this participation ratio is comparable to N . We now investigate the case of disordered materials. The correlation between disorder, exciton localization, and distance from the interface and dissociation rates is shown in Fig. 3. The spatial extent of the Frenkel states is characterized by the horizontal and vertical coordinates: the x axis shows the average position within the donor chain while the vertical axis gives the participation

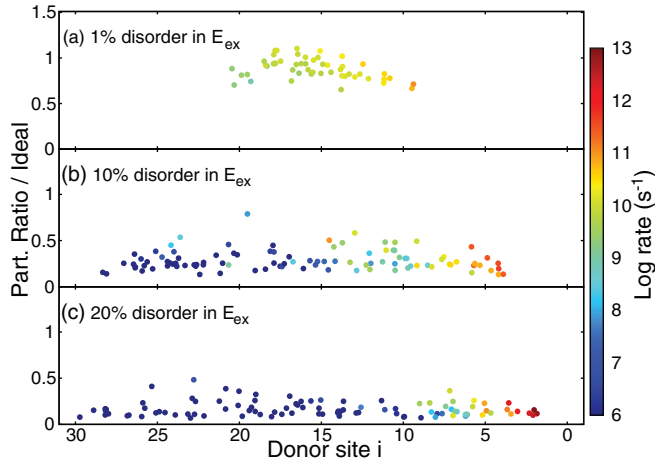


FIG. 3. (Color online) Exciton dissociation rates for disorder in the Frenkel parameter E_{ex} for a chain of 30 donors and 30 acceptors (to the right of the figure starting at site 0, not shown) as a function of the average position i_{av} and participation ratio scaled to its value for ideal systems. The color gives the logarithm of the dissociation rate.

ratio scaled to the value for ideal chains given above. The color shows the logarithm of the exciton dissociation rate (at $E = \epsilon_{n=1}$). Materials with low (e.g., 1%) disorder [Fig. 3(a)] result in a narrow range of dissociation rates with Frenkel states that are delocalized over the donor having i_{av} at the center of the chain and participation ratios comparable to the size of the donor system. Here long-range dissociation can take place since Frenkel wave functions have maximal amplitude at the center of the donor material yet sufficient weight at the interface. For the parameters used, dissociation rates are $\sim 10^{10} \text{ s}^{-1}$ which correspond to exciton lifetimes of $\sim 15 \text{ ps}$.

Disorder in the donor material localizes the excitons and their distance to the interface then becomes critical in determining their dissociation rate, as shown in Figs. 3(b) and 3(c). Excitons to the left of Fig. 3 are far from the interface [Fig. 1(a)] and have very low dissociation rates since they have negligible amplitudes on the interface site and are therefore poorly coupled to CT states [Eq. (7)]. The opposite is true for excitons close to the acceptor. In these disordered systems dissociation rates can span many orders of magnitude. In most cases rates are lower than in the ideal case but rates as high as $\sim 10^{13} \text{ s}^{-1}$ ($\tau \sim 15 \text{ fs}$) are obtained for 20% disorder. The subpicosecond dissociation rates reported in most experiments^{15–17} are clearly due to excitons close to the interface.

The top panels in Fig. 4 show the exciton dissociation rates as a function of the average donor site i_{av} for several degrees of disorder in the parameters E_{ex} or J that describe the Frenkel on-site energy. Each set consists of 100 disordered “samples.” The rates span a wide range of values, especially for the case of high (20%) disorder, but a clear trend can be seen. To quantify the distance dependence of the CT generation rates we fit all data to an exponential function of the form $A e^{-\beta i}$, where i labels the donor sites, A is a prefactor, and β is the distance decay constant.

We find that β increases linearly with amount of disorder in the Frenkel states, as shown in Fig. 5. We also find that additional disorder in CT state parameters has little effect on

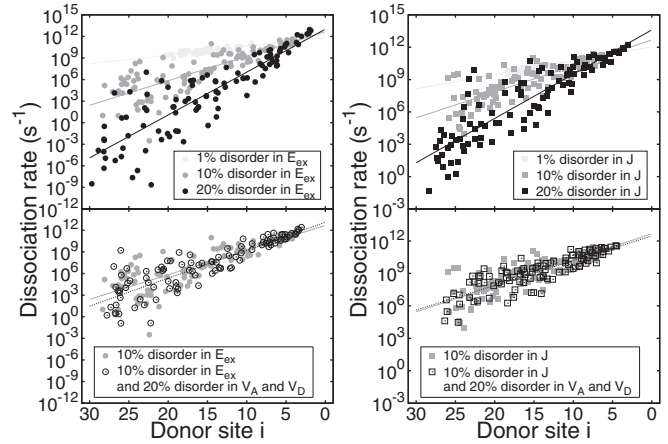


FIG. 4. Exciton dissociation rates as a function of i_{av} for systems with different degrees of disorder in the Frenkel on-site energy E_{ex} (left) or in the exciton coupling J (right). The bottom panels compare the results for an additional 20% disorder in CT parameters V_A and V_D . Lines are exponential fits, as described in the text.

the dissociation rates: adding 20% disorder in V_A and in V_D to a system with 10% of disorder in E_{ex} results in dissociation rates spanning a similar range of values while the exponential fitted slope β is unaffected (Fig. 4, bottom panels). The smaller role of disorder in CT states is due to the large (N^2) number of CT states, which are closely spaced in the energy of the Frenkel state. Disorder in V_A and V_D does not alter the CT density of states in a significant way (see inset of Fig. 5) and exciton dissociation rates are almost unaffected.

Importantly, regardless of the disorder the exciton dissociates into partially separated hole and electrons suggesting that the essential physics of free hole and electron generation is unaffected by the chemical details of the interface.

The exponential dependence of exciton dissociation rates with exciton-interface distance is similar to what has been observed in donor/bridge/acceptor molecular systems and families of molecular wires of different lengths.^{30–32} Here,

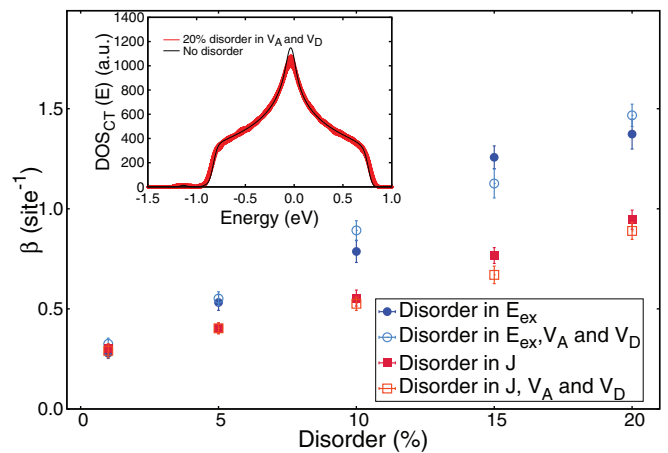


FIG. 5. (Color online) Distance decay constant β as a function of disorder. Error bars correspond to the standard error. Additional 20% disorder in the CT state parameters V_A and V_D (open symbols) has a minor impact on β . Inset: CT DOS for no disorder (black) and for 100 “samples” with 20% disorder in V_A and V_D (red).

however, there is no chemical (or conceptual) distinction between the donor and bridge as they are both part of the same disordered Hamiltonian and therefore one cannot use the language of superexchange to describe the effective coupling between states localized by disorder and acceptor states.³³ Instead, in this approach the exponential behavior comes out in a seamless way from the wave function localization induced by the introduction of disorder.

V. CONCLUSIONS

In summary, we have proposed a methodology that describes clearly and compactly the process of exciton dissociation at organic photovoltaic cells. Regardless of the level of disorder of the donor or acceptor materials the final state is invariably a partially charge separated state as the bound CT state is too low in energy to be directly populated by

the exciton on the donor. The same methodology, virtually with no additional work, illustrates the role of disorder in donor and acceptor materials and provides a compact description of the dependence of exciton dissociation with distance from the interface. This approach, rooted in the theory of molecular junctions, explores the essential physics of charge separation and seems ideal, if coupled to more detailed atomistic description of the interface, to study the correlation between the local structure and the charge generation quantum yield.

ACKNOWLEDGMENTS

We gratefully acknowledge financial support from the ERC (Microscopic Modelling of Excitonic Solar Cells Interfaces). We thank Emanuele Maggio for fruitful discussions.

*vazquez@fzu.cz

†a.troisi@warwick.ac.uk

¹C. Deibel, T. Strobel, and V. Dyakonov, *Adv. Mater.* **22**, 4097 (2010).

²H. Ohkita, S. Cook, Y. Astuti, W. Duffy, S. Tierney, W. Zhang, M. Heeney, I. McCulloch, J. Nelson, D. D. C. Bradley *et al.*, *J. Am. Chem. Soc.* **130**, 3030 (2008).

³S. H. Park, A. Roy, S. Beaupre, S. Cho, N. Coates, J. S. Moon, D. Moses, M. Leclerc, K. Lee, and A. J. Heeger, *Nat. Photonics* **3**, 297 (2009).

⁴C. L. Braun, *J. Chem. Phys.* **80**, 4157 (1984).

⁵P. Peumans and S. R. Forrest, *Chem. Phys. Lett.* **398**, 27 (2004).

⁶X.-Y. Zhu, Q. Yang, and M. Muntwiler, *Acc. Chem. Res.* **42**, 1779 (2009).

⁷M. Wiemer, A. V. Nenashev, F. Jansson, and S. D. Baranovskii, *Appl. Phys. Lett.* **99**, 013302 (2011).

⁸S. R. Yost, L.-P. Wang, and T. Van Voorhis, *J. Phys. Chem. C* **115**, 14431 (2011).

⁹A. V. Nenashev, S. D. Baranovskii, M. Wiemer, F. Jansson, R. Österbacka, A. V. Dvurechenskii, and F. Gebhard, *Phys. Rev. B* **84**, 035210 (2011).

¹⁰J.-L. Brédas, J. E. Norton, J. Cornil, and V. Coropceanu, *Acc. Chem. Res.* **42**, 1691 (2009).

¹¹K. Vandewal, K. Tvingstedt, A. Gadisa, O. Inganäs, and J. V. Manca, *Nat. Mater.* **8**, 904 (2009).

¹²T. M. Clarke and J. R. Durrant, *Chem. Rev.* **110**, 6736 (2010).

¹³A. Troisi, *Faraday Discuss.* **163**, 377 (2013).

¹⁴M. Muntwiler, Q. Yang, W. A. Tisdale, and X.-Y. Zhu, *Phys. Rev. Lett.* **101**, 196403 (2008).

¹⁵A. A. Bakulin, A. Rao, V. G. Pavelyev, P. H. M. van Loosdrecht, M. S. Pshenichnikov, D. Niedzialek, J. Cornil, D. Beljonne, and R. H. Friend, *Science* **335**, 1340 (2012).

¹⁶A. E. Jailaubekov, A. P. Willard, J. R. Tritsch, W.-L. Chan, N. Sai, R. Gearba, L. G. Kaake, K. J. Williams, K. Leung, P. J. Rossky *et al.*, *Nat. Mater.* **12**, 66 (2013).

¹⁷G. Grancini, M. Maiuri, D. Fazzi, A. Petrozza, H.-J. Egelhaaf, D. Brida, G. Cerullo, and G. Lanzani, *Nat. Mater.* **12**, 29 (2013).

¹⁸F. C. Spano, *Acc. Chem. Res.* **43**, 429 (2010).

¹⁹S. Datta, *Quantum Transport: Atom to Transistor* (Cambridge University Press, Cambridge, 2005).

²⁰H. Haug and A. P. Jauho, *Quantum Kinetics in Transport and Optics of Semiconductors*, Springer Series in Solid-State Sciences, Vol. 123 (Springer, Berlin, Heidelberg, New York, 2006).

²¹P. F. Barbara, T. J. Meyer, and M. A. Ratner, *J. Phys. Chem.* **100**, 13148 (1996).

²²G. D. Scholes, *ACS Nano* **2**, 523 (2008).

²³S. S. Zade and M. Bendikov, *Chem. Eur. J.* **14**, 6734 (2008).

²⁴A. Troisi, *Chem. Soc. Rev.* **40**, 2347 (2011).

²⁵F. May, B. Baumeier, C. Lennartz, and D. Andrienko, *Phys. Rev. Lett.* **109**, 136401 (2012).

²⁶S. Westenhoff, W. J. D. Beenken, A. Yartsev, and N. C. Greenham, *J. Chem. Phys.* **125**, 154903 (2006).

²⁷I. A. Howard, R. Mauer, M. Meister, and F. Laquai, *J. Am. Chem. Soc.* **132**, 14866 (2010).

²⁸J. Guo, H. Ohkita, H. Benten, and S. Ito, *J. Am. Chem. Soc.* **132**, 6154 (2010).

²⁹D. P. McMahon, D. L. Cheung, and A. Troisi, *J. Phys. Chem. Lett.* **2**, 2737 (2011).

³⁰B. Albinsson and J. Mårtensson, *J. Photochem. Photobiol. C* **9**, 138 (2008).

³¹I. A. Balabin, D. N. Beratan, and S. S. Skourtis, *Phys. Rev. Lett.* **101**, 158102 (2008).

³²Y. A. Berlin, F. C. Grozema, L. D. A. Siebbeles, and M. A. Ratner, *J. Phys. Chem. C* **112**, 10988 (2008).

³³S. Skourtis and A. Nitzan, *J. Chem. Phys.* **119**, 6271 (2003).

³⁴C.-P. Hsu, *Acc. Chem. Res.* **42**, 509 (2009).

³⁵The coupling (excitonic and hopping integrals) is consistent with the typical range observed in molecular materials (see, e.g., Ref. 34). C was set to the Coulombic attraction between two elementary charges 5 Å apart (a typical distance between molecules in crystals) in a dielectric environment with $\epsilon = 3$.